Aerosol and Air Quality Research

Modeled Respiratory Tract Deposition of Smoke Aerosol from Conventional Cigarettes, Electronic Cigarettes and Heat-not-burn Products

Yawen Li[1], Huapeng Cui[1*], Li Chen[1], Meijuan Fan[1], Junlan Cai[1], Junwei Guo[1], Caner U. Yurteri[2], Xiaoxi Si[3], Shaofeng Liu[1], Fuwei Xie[1], Jianping Xie[1]

[1] Zhengzhou Tobacco Research Institute of CNTC, Zhengzhou, China
[2] Research and Development, British American Tobacco Investments Ltd, Regents Park Road, Southampton, Hampshire SO15 8TL, UK
[3] RandD Center of China Tobacco Yunnan Industrial Co., Ltd., Kunming, China

ABSTRACT

Knowledge of the deposition of inhaled smoke aerosol in the human respiratory tract has great value for risk assessments of the inhalation toxicology of tobacco products. In this study, differential mobility spectrometry (DMS) was used to characterize smoke particles generated from a conventional cigarette, e-cigarette and heat-not-burn product. The aerosol properties obtained by DMS were then applied to a Multiple Path Particle Dosimetry (MPPD) model to predict the deposition of aerosol particles in the human respiratory tract. The DMS results showed that the particle size distribution of aerosol from the three products differed considerably, with a count median diameter of 14.2–25.4 nm, 50.6–55.3 nm and 172–179 nm for the e-cigarette, heat-not-burn product and conventional cigarette, respectively. However, there was no significant difference in the particle number concentration of aerosol from the three products. The MPPD model indicated that the total deposition fraction of aerosol particles from the e-cigarette and heat-not-burn product was higher than that from the conventional cigarette, and deposition of particles from the e-cigarette in the three human airway regions (head airway, tracheobronchial and pulmonary regions) was higher than that from the heat-not-burn product and conventional cigarette; the particle number concentration deposited in the pulmonary region was the highest, comprising more than 60% of total deposition. Lastly, among the lung lobes, the highest number deposition fraction occurred in the right lower lobe. The relationship between deposition fraction and airway generation was relatively similar among the three aerosols, and the highest deposition fraction occurred in the 20th to 23rd generation airways. The deposition results showed that smaller particles, such as those from the e-cigarette aerosol, were more easily deposited in the human respiratory tract. Combined with knowledge of the harmful aerosol constituents, these deposition data will provide important information for hazard evaluation of new tobacco products.

Keywords: Conventional cigarette, E-cigarette, Heat-not-burn product, Aerosol property, Respiratory tract, MPPD-modeled deposition

1 INTRODUCTION

Numerous studies have confirmed the health risks of cigarette smoking, which is generally considered to be the leading preventable cause of various diseases, such as lung cancer, cardiovascular disease and stroke (Church *et al.*, 2009; Barua and Ambrose, 2013; Hackshaw *et al.*, 2018; WHO, 2008). The pathogenic substances mainly stem from the cigarette smoke generated by tobacco consumption. There are more than 7000 chemical constituents in cigarette smoke (Rodgman and Perfetti, 2008), including hundreds of toxins and carcinogens (Baker, 2006;

Geiss and Kotzias, 2007). In recent years, new types of product have emerged in the tobacco market. In particular, products such as e-cigarettes and heat-not-burn (HnB) products are becoming increasing popular owing to their claimed function of being able to reduce or even eliminate toxicity or mutagenicity of cigarette smoke (Chen, 2017; Simonavisius *et al.*, 2018; Boue *et al.*, 2020).
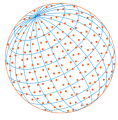
It is the chemicals carried by smoke particles that are associated with disease (U.S. Department of Health and Human Services, 2014). However, it is insufficient to assume that the lower yield of chemical components produced by new tobacco products is less harmful. In general, cigarette smoke particles are typically sub-micron and easily deposited in the human respiratory tract during smoking. The physical properties of the aerosol are likely to affect the deposition of particles and further affect the retention of chemicals, which is an important aspect of the health risks of smoking. Furthermore, smaller particles may be deposited more deeply in the human respiratory tract (Carvalho *et al.*, 2011). Therefore, smoke exposure and hazard evaluation should not only focus on the chemicals, but also account for the deposition of aerosol particles.

A few studies have investigated the deposition of environmental or smoke aerosol particles in human airways. For example, Martins *et al.* (2010) simulated the deposition of atmospheric fine particles in the human airway. Patterson *et al.* (2014) also evaluated the deposition of environmental ultrafine particles in the respiratory tracts of school-aged children. Regarding smoke aerosol, Zhe *et al.* (2012) analyzed the deposition of cigarette smoke particles in the human upper airways, Zhang *et al.* (2012), Pichelstorfer *et al.* (2016) and Sosnowski *et al.* (2016) predicted the deposition of smoke particles from e-cigarettes and conventional cigarettes. Moreover, Protano *et al.* (2017) investigated the second-hand smoke generated by conventional cigarettes, e-cigarettes and HnB products.

Those studies have provided a better understanding of particle deposition in the respiratory tract. To our knowledge, however, there has been no comprehensive comparison of the deposition of smoke particles between conventional cigarettes and modern tobacco products (e-cigarettes and HnB products) as yet, especially in terms of number concentration (NC) deposition in the regional and whole airways. As compared with conventional cigarettes, the aerosol generated from e-cigarettes and HnB products may have different physical properties, leading to different doses of respiratory deposition. Thus, it is necessary and significant to determine the physical properties of aerosol particles from these products, and use them to estimate the deposition dose of particles in the human airways, which might be applied to comprehensive assessment of the health risks of new tobacco products.

The physical properties of an aerosol, including particle NC, count median diameter (CMD) and geometric standard deviation (GSD) among others, are important parameters for estimating the deposition dose of the particles. To predict the deposition of the smoke particles in the human respiratory tract, therefore, these physical properties must be measured accurately (Kane *et al.*, 2010; Sahu *et al.*, 2013). Methods for the characterization of smoke particles have been developed since the 1970s. Kijowski (1985) reviewed early approaches to smoke particle size, including microscopy (Holmberg and Yeatts, 1976), centrifugation (Hinds, 1978), an aerodynamic particle sizer (McCusker *et al.*, 1982), and a light scattering technique (Leaderer *et al.*, 1984), among others. More recently, differential mobility spectrometry (DMS) has been developed for real-time measurements of the particle size distribution of cigarette smoke (Adam *et al.*, 2009; Alderman and Ingebrethsen, 2011; Cui *et al.*, 2020). DMS is based on the difference in electro migration of charged particles in an electric field, and can be used to measure both particle number and particle size distribution, as described in detail by Symonds *et al.* (2007).

Using DMS, Adam (2009) reported that cigarette smoke aerosol has a CMD of 180−280 nm, and a particle NC of 1.4×10^9 to 1.5×10^{10} N cm^{-3}. Alderman and Ingebrethsen (2011) combined DMS with a smoking cycle simulator (SCS) to characterize the smoke aerosol from 29 different brands of cigarettes under intense (puff volume 60 mL, duration 2 s, puff interval 30 s) and standard (puff volume 35 mL, duration 2 s, puff interval 30 s) smoking regimes, reporting that the CMD of particles generated under the intense smoking regime was 145–189 nm, which was 12–22 nm smaller than that generated under the standard smoking regime. Duan *et al.* (2015) compared the smoke aerosol particles of conventional cigarettes and e-cigarettes by DMS, showing that the particle size of e-cigarette aerosols was smaller than that of conventional cigarettes. Similarly, Si *et al.* (2018) investigated the physical properties of HnB aerosols, finding

that the particle size of HnB aerosol was smaller than that of conventional cigarette smoke.

Regarding particle deposition, various computational models have been formulated to predict the respiratory-tract dosimetry of inhaled particles. These models are generally mathematically complex and multidisciplinary. Many are based on a lung structure constructed from actual airway measurements, combined with experimental investigations and a series of calculations to predict particle deposition, such as Computational Fluid–Particle Dynamics (CF-PD) simulation models (Rostami, 2009; Kleinstreuer and Zhang, 2010; Hofmann, 2011; Sosnowski, 2011; Kleinstreuer and Feng, 2013), the ICRP dosimetry model (Bair, 1995; Mellat *et al.*, 2017) and the Multiple Path Particle Dosimetry (MPPD) model (Martins *et al.*, 2010; Li *et al.*, 2016). Among these models, the MPPD model is based on realistic lung geometry, physiology and deposition mechanisms, and it provides estimates of both the whole-lung and the regional particle deposition fractions that have been validated with experimental data (Rostami, 2009). In addition, the MPPD dosimetry model is freely available to the public (http://www.ara.com/products/mppd.htm), and has user-friendly menu-driven selections to aid input of the study variables (Anjilvel and Asgharian, 1995; Miller *et al.*, 2016).

The MPPD model has been used to estimate the deposition of inhaled particles in different regions of the human respiratory tract. For example, Liang *et al.* (2017) employed a wide-range particle spectrometer to characterize smoke aerosols and applied the data to the MPPD model to analyze the deposition fraction and concentration of fine particles in various regions of the human respiratory system. Sahu *et al.* (2013) used the MPPD model to study the deposition fraction of cigarette smoke in the human head airway, and tracheobronchial and alveolar regions. In addition, Manigrasso *et al.* (2015) carried out a detailed investigation into the deposition distribution of e-cigarette aerosol in human alveoli based on the MPPD model.

As mentioned above, comprehensive health risk assessment of tobacco products should also consider the deposition of aerosol particles in the human airways. In this paper, therefore, the physical properties of aerosols from conventional cigarettes, e-cigarettes, and HnB products were measured by SCS-DMS and the results were applied to the MPPD model to evaluate the regional and total distribution of aerosol particles deposited in the human respiratory tract.
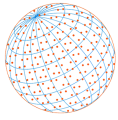
2 MATERIALS AND METHODS

2.1 Samples

In total, nine commercially available tobacco products were assessed in this study, including conventional cigarettes with different tar content (n = 3), and different types of e-cigarettes (n = 3) and HnB products (n = 3). Information on the nine products is summarized in Table 1.

The conventional cigarettes were conditioned at 22 ± 1°C and 60 ± 3% relative humidity (RH) for more than 48 hours before analysis; the e-cigarettes and HnB products were test directly after being taken out of the package. Measurements were performed under the ambient laboratory conditions at 24 ± 3°C and 45 ± 5% RH.

Table 1. Tobacco products analyzed in this study.

Product No.	Details
Conventional cigarette	
#1 (3R4F)	Tar 9.4 mg
#2	Tar 5.0 mg
#3	Tar 11.0 mg
E-cigarette	
#4	Disposable
#5	Cartomizer
#6	Rechargeable
Heat-not-burn product	
#7	Internal heating
#8	Internal heating
#9	External heating

2.2 Smoke Aerosol Characterization

The properties of the aerosol generated by all products were measured by an SCS-DMS system (Fig. 1), which has been previously described in detail by Alderman and Ingebrethsen (2011). In brief, the SCS is used to simulate various puff profiles and to accurately control the flow rate, while DMS is used to measure the particle NC and size distribution of the aerosol. The instrument has 38 channels and can classify particle size ranging from 5 to 1000 nm.

For the conventional cigarettes and HnB products, the ISO puffing regime (bell profile; puff volume, 35 mL; puff duration, 2 s; puff interval, 60 s) (ISO, 2000) was used; for the e-cigarettes, the ISO puffing regime (square profile; puff volume, 55 mL; puff duration, 3 s; puff interval, 30 s) (ISO 20768: 2018) was used. The following conditions were used: initial sampling flow rate of SCS-DMS, 25 L min^{-1}; sampling flow rate of DMS, 8 L min^{-1}; secondary dilution ratio, 1:200; sampling head temperature, 40°C; sheath gas temperature, 40°C; cyclone separator temperature, 80°C; acquisition frequency of DMS, 10 Hz. All products were tested under these experimental conditions.

2.3 MPPD-modeled Particle Deposition

To predict the deposition of aerosol particles in the human respiratory tract, the DMS aerosol data (i.e., NC, CMD, GSD) of the samples were averaged and entered into MPPD version 3.04, a computational model jointly developed by the American Hamna Health Research Institute and the National Institute of Public Health and Environment of the Netherlands. MPPD can calculate particle deposition in the respiratory tract of humans (adults and children), rats, pigs and monkeys for monodisperse and polydisperse aerosols with particle sizes ranging from 0.001 to 100 μm, and its detailed function is described on its official website.

The modeled deposition is based on single-path or multiple-path methods for tracking air flow and calculating aerosol deposition in the lung. In this study, the multiple-path method was chosen because it essentially reflects the real structure of the human respiratory system, as explained in detail by Anjilvel and Asgharian (1995). For the human lung, there are several options for lung geometry, including Yeh–Schum single path, Yeh–Schum 5-lobe, stochastic model, age-specific symmetric model, age-specific 5-lobe model, Weibel symmetric model, PNNL symmetric model, and PNNL asymmetric model. On the basis of published reports (Roy *et al.*, 1991; Li *et al.*, 2016), the stochastic model was employed with lung size set at the 60th percentile to predict the aerosol distribution and deposition in the Chinese adult respiratory tract. The following parameters were applied to MPPD: functional residual air volume, 2950 mL; upper respiratory tract volume, 44.7 mL;
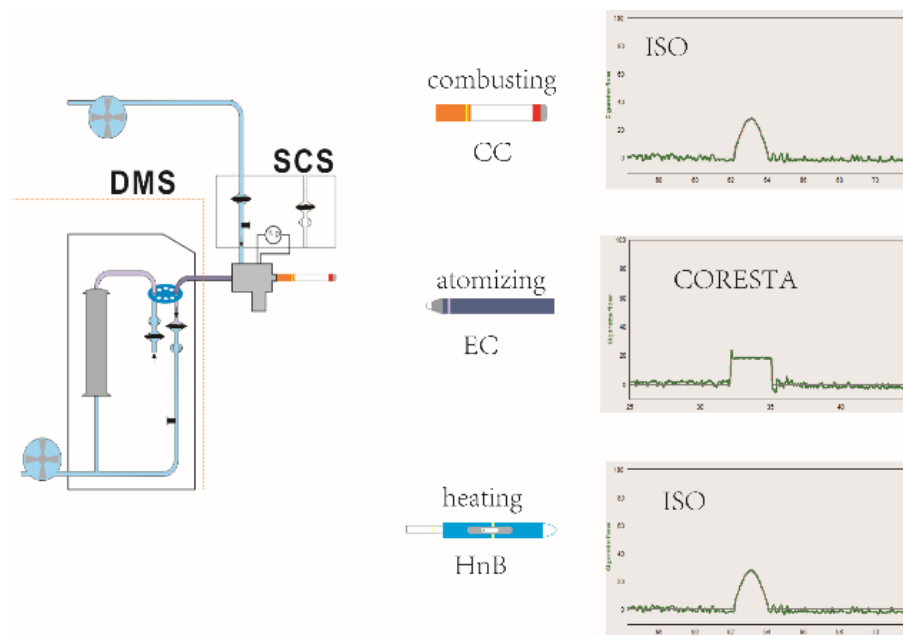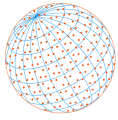

Fig. 1. Schematic diagram showing the characterization of aerosol from a conventional cigarette (CC), e-cigarette (EC) and heat-not-burn (HnB) product under different smoking regimes.

tidal volume, 537.5 mL. The duration of a single puff was set as 5 s with 2 s inhalation, 1 s pause, and 2 s exhalation, and the breathing condition was set as oral breathing. The other parameters were the default values in the model.

DMS provides the size distributions of aerosol particles in terms of particle electrical mobility diameter and NC (N cm^{-3}); however, the input data for the MPPD model needs to be particle aerodynamic diameter. Previously, Hinds (1999) proposed Eq. (1) to convert particle electrical mobility diameter to aerodynamic diameter:

$$D_a = D_m \sqrt{\chi C_s (D_m) \rho_p / C_s (D_a) \rho_0} \tag{1}$$

where D_a and D_m are the particle aerodynamic diameter (nm) and particle electrical mobility diameter (nm), respectively; χ is the shape factor, C_s is the Cunningham slip correction factor for a certain diameter; ρ_p is the density of the particles and ρ_0 is the reference density (1 g cm^{-3}). The shape factor is assumed as 1 for spherical cigarette smoke particles (Johnson *et al.*, 2015). Both the electrical mobility diameter and aerodynamic diameter require correction, and the correction factors are found to be similar. The Cunningham slip factor is neglected. We estimated the error introduced by neglecting the Cunningham slip factor to be 8% for particles smaller than 10 nm, a maximum of 5% for particle sizes between 10 and 50 nm, a maximum of 3% for particle sizes between 50 and 100 nm, and smaller than 1% for particles larger than 500 nm. Therefore, neglection will not introduce a significant error for particle sizes larger than 1 μm. Thus, the relationship between D_m and D_a will become:

$$D_a = D_m \sqrt{\rho_p} \tag{2}$$

The effective density of cigarette smoke particles is 1.18 g cm^{-3} (Johnson *et al.*, 2015). Thus,

$$D_a = 1.09 \times D_m \tag{3}$$

Therefore, the particle aerodynamic diameter is used to discuss our findings (except for the DMS measurement data).

To our knowledge, however, there are no reports of the effective density of aerosol particles from e-cigarettes or HnB products. The aerosol from an e-cigarette mainly comprises glycerol (ρ, 1.26 g cm^{-3}) and propylene glycol (ρ, 1.03 g cm^{-3}), whereas that from an HnB product comprises glycerol and other tobacco constituents. Approximately, therefore, the effective density of aerosol particles among the three products should be similar. Therefore, a ρ_p value of 1.18 g cm^{-3} was used for MPPD modeling in this study.

The aerosol particle hygroscopic growth, evaporation-coagulation (Asgharian *et al.*, 2014, 2018; Sosnowski and Odziomek, 2018) and the colligative motion (Broday and Robinson, 2003) of concentrated aerosols have a certain influence on local particle deposition in the respiratory system; however, it should be noted that the MPPD modeled deposition here focused on a comparison of the three kinds of tobacco product. The estimation produced by the modeling process is based on a few assumptions and neglection of thermodynamic and kinetic reactions (e.g., hygroscopic growth and coagulation).

3 RESULTS AND DISCUSSION

3.1 Physical Properties of the Aerosol from Conventional Cigarettes, e-cigarettes, and HnB Products

Initially, the physical properties of three different sample aerosols were measured by SCS-DMS over a puff number of 6, 10, and 6 for one conventional cigarette (#1, 3R4F, a standard reference cigarette developed by the University of Kentucky Centeror Tobacco Reference Products that is used throughout the tobacco industry and academic laboratories as a consistent and uniform test item for inhalation toxicology research), one e-cigarette (#4), and one HnB product (#7), respectively. The DMS data showed that the CMD and GSD of the three products remained
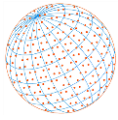
essentially the same across the puffs; and the NC of the 3R4F cigarette and HnB product tended to increase with puff number, while that of e-cigarette did not vary with puff number (Fig. S1–S3). The increase of particle number concentration for 3R4F cigarette was due to the decreased filtering effect of the tobacco rod with puff number (Adam *et al.*, 2009). For HnB product, the increase of particle number concentration was attributed to the increase in temperature of the heater with puff number. For e-cigarette, the power for atomization of e-liquid was fixed for each puff, which keeps constant atomization temperature and produces the same aerosol.

Fig. 2 shows the puff-by-puff particle size distribution of aerosol from the 3R4F cigarette, e-cigarette and HnB product. In general, the aerosols of the 3R4F cigarette, e-cigarette and HnB all showed a single-peak log-normal distribution, and this distribution did not vary significantly variation among the puffs taken. For 3R4F, the particle size of the smoke was mainly concentrated in the range 50–600 nm, and was close to 200 nm at the peak concentration. The concentration of smoke particles tended to increase with increasing puff number. For the e-cigarette, the particle size of the aerosol was in the range 5–150 nm, and was close to 20 nm at the highest concentration; unlike 3R4F, the concentration of aerosol particles did not change significantly with increasing the puff number. Lastly, the particle size of the HnB aerosol was mainly concentrated in range 10–200 nm, and was close to 50 nm at the highest concentration; similar to 3R4F, the concentration of aerosol particles showed an increasing trend with increasing puff number.

All nine tobacco products were subjected to SCS-DMS; for each product, the results for each puff were averaged to obtain the mean physical properties of the aerosol (Table 2). The NC of aerosol particles ranged from 4.55×10^9 to 1.12×10^{10} N cm^{-3} for conventional cigarettes, 5.75×10^9 to 8.27×10^9 N cm^{-3} for e-cigarettes, and 1.23×10^9 to 8.01×10^9 N cm^{-3} for HnB products. Overall, the NC of aerosol particles varied greatly among different products, thus, it seems more likely that NC is related to the design parameters of the product itself.

There was a more obvious difference in particle size among the three product types with size increasing in the following order: e-cigarettes (CMD, 14.2–25.4 nm) < HnB cigarettes (CMD, 50.6–55.3 nm) < conventional cigarettes (CMD, 172–179 nm). This trend is mainly due to differences in the mechanism of aerosol generation of the three product types. Conventional cigarette tobacco has a high combustion temperature and the smoke contains a large quantity of solid particles and high-boiling-point organics, which can readily to form relatively large particles. The temperature of tobacco in the HnB product typically reaches 200–350°C during the heating process; at this temperature, volatile and semi-volatile organic compounds in the tobacco matrix are released, which form relatively small particles during the process of condensation. During aerosol formation in e-cigarette, the e-liquid completely vaporizes and then condenses into tiny droplets. Because the atomization process does not produce solid particles and the nucleation rate of the minute droplets is slow, the particle size is smaller for e-cigarettes. Lastly, there was no obvious difference in GSD among the three product types.

3.2 Deposition of Aerosols in the Human Respiratory Tract

To predict the deposition and distribution of aerosol particles in the human respiratory tract, the aerosol properties determined for one of each product type were applied to the MPPD model: convention cigarette #1 (3R4F), e-cigarette #4 and HnB product #7. For these three products, the particle NC of aerosol was 8.35×10^9, 6.14×10^9 and 8.01×10^9 N cm^{-3}, respectively; the CMD was 172, 25.4 and 55.3 nm, respectively; and the GSD was 1.41, 1.77 and 1.53, respectively. For the density of cigarette smoke particles, we used the value of 1.18 g cm^{-3} reported by Johnson *et al.* (2015), and assumed that this value would be valid for the density of aerosol particles generated from the e-cigarette and HnB product.

3.3 Deposition of Aerosol in Different Regions of the Human Respiratory Tract

The above DMS measurements showed that the particle size of aerosol from the three products ranged from 1 nm (e-cigarette) to 1 μm (conventional cigarette). As shown in Fig. 3, the MPPD deposition model shows that the particle size of an aerosol plays an important role in the total deposition and the deposition fractions in different regions of the human respiratory tract. For example, the deposition fraction of particles ranging from 20 to 1000 nm is higher in the pulmonary region than in tracheobronchial region or head region.
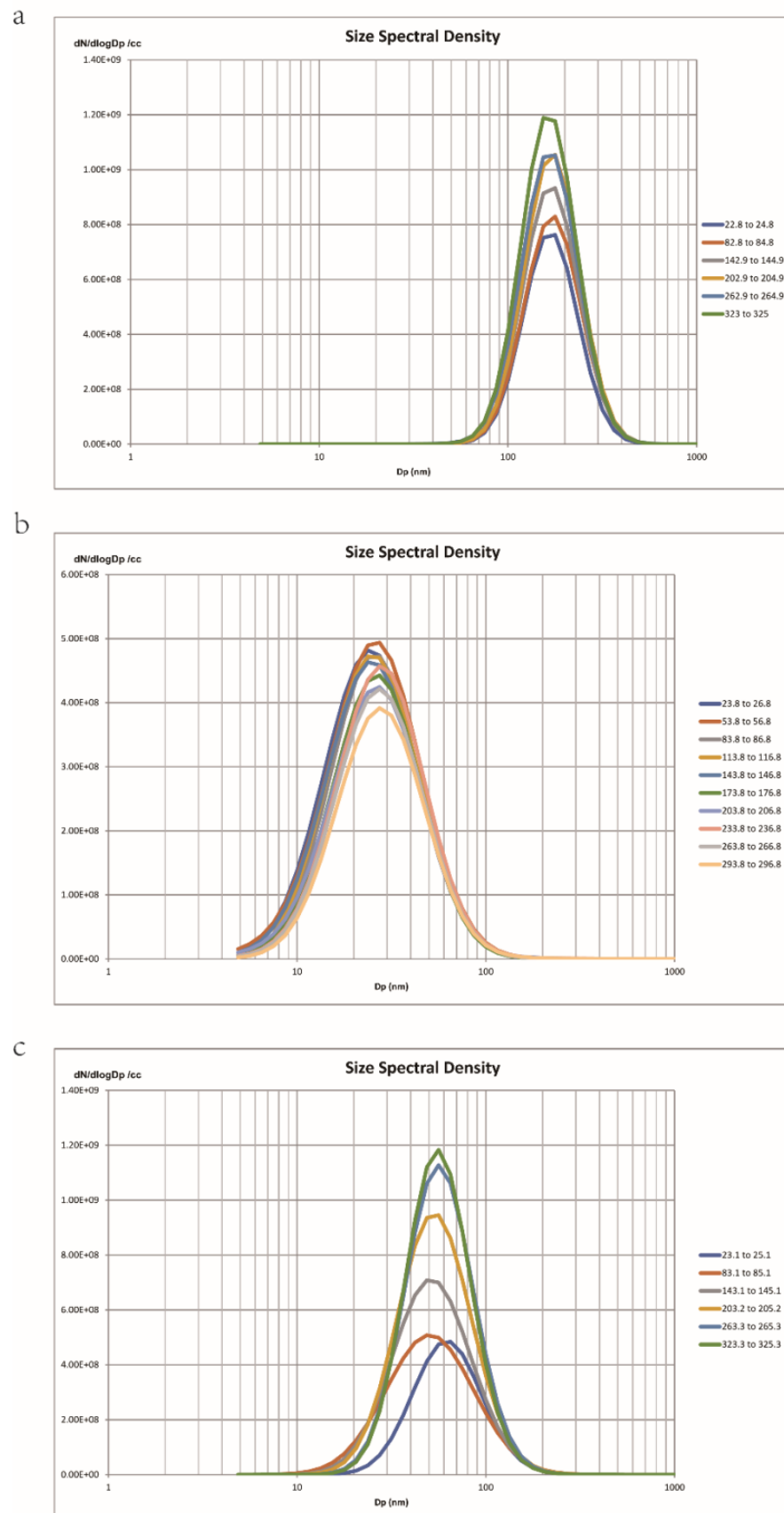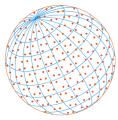
Fig. 2. Puff-by-puff particle size distribution in mainstream aerosol from three different tobacco products. (a) CC #1 (3R4F); (b) EC #4; (c) HnB #7. The numbers in the key indicate the time when each 2-s puff was taken.
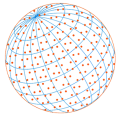
Table 2. Particle NC and distribution data of the aerosol generated by the three products.

Product	Particle NC (N cm^{-3})	CMD (nm)	GSD
Conventional cigarette			
#1 (3R4F)	8.35×10^9	172	1.41
#2	4.55×10^9	177	1.43
#3	1.12×10^{10}	179	1.43
E-cigarette			
#4	6.14×10^9	25.4	1.77
#5	8.27×10^9	22.3	1.86
#6	5.75×10^9	14.2	1.60
Heat-not-burn product			
7#	8.01×10^9	55.3	1.53
8#	4.71×10^9	55.0	1.62
9#	1.23×10^9	50.6	2.55

Abbreviations: CMD, count median diameter; GSD, geometric standard deviation; NC, number concentration.
All data were puffs averaged.
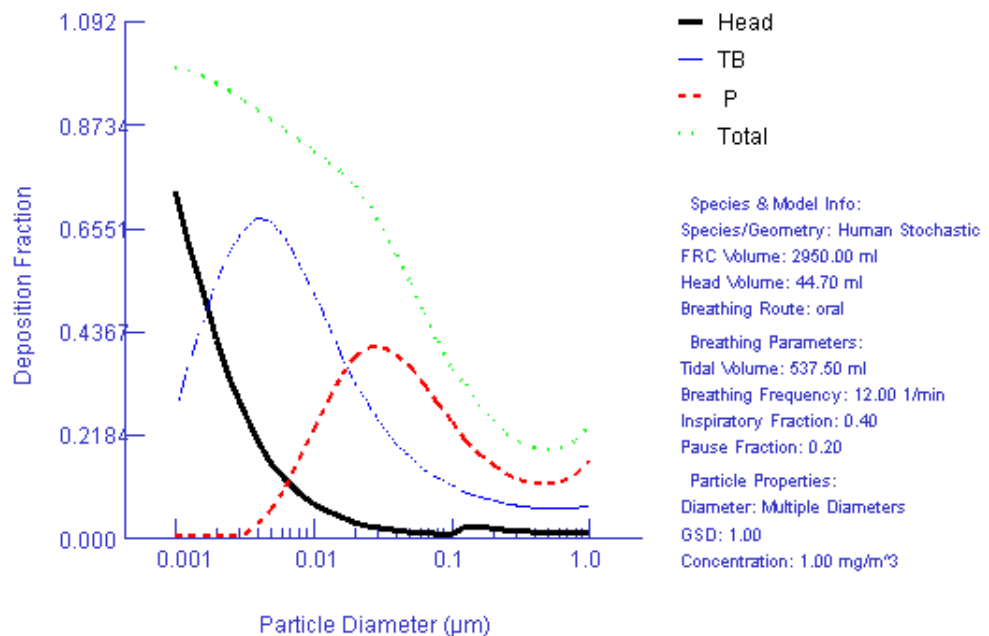Convential cigarette: n = 3, 6 puffs; e-cigarette: n = 3, 10 puffs; heat-not-burn product: n = 3, 6 puffs.

Fig. 3. MPPD-modeled deposition fraction of aerosol in different respiratory regions by particle size. Abbreviations: TB, tracheobronchial region; P, pulmonary region.

The deposition fraction of aerosol particles from the three kinds of tobacco product in different regions of the human respiratory tract is shown in Fig. 4. For all three products, the fraction of particle deposition in the various regions showed the trend: head airway < tracheobronchial region < pulmonary region. The deposition fraction in the head was the lowest, accounting for 4.0%–6.2% of the total airway deposition. Deposition in this region would be mainly due to the diffusion of aerosol particles in the oral cavity. As the aerosol is drawn into the tracheobronchial region, the passage narrows, causing the flow rate to increase, and as a result particle deposition increases. Deposition in this region accounted for ~30% of the total airway deposition. When the aerosol enters the lungs, the closer contact with the pulmonary alveoli and the narrower and longer moving path further increases particle deposition; particle deposition in the alveoli accounted for about 60% of the total airway deposition.
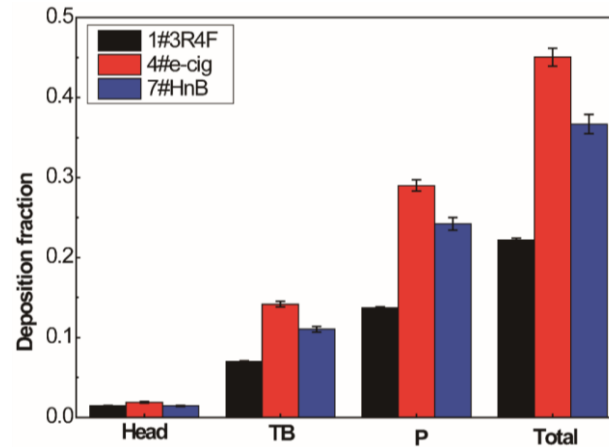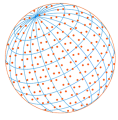
Fig. 4. Fraction of deposition in the head airways, tracheobronchial (TB) region and pulmonary (P) region, and total deposition of aerosol particles from the CC, EC and HnB.

Regarding the three tobacco products, the e-cigarette aerosol had the highest deposition fraction both in total and in each of the three respiratory regions. Deposition in the head airways followed the order: e-cigarette > conventional cigarette > HnB product; and deposition in the tracheobronchial and pulmonary regions, and in total followed the order: e-cigarette > HnB product > 3R4F cigarette. Moreover, the total deposition fraction of the e-cigarette aerosol was 1.23 times that of the HnB product, and 2.03 times that of the conventional cigarette. Therefore, the e-cigarette has a higher deposition fraction in the human respiratory tract relative to the HnB product and conventional cigarette, which is mainly due to the particle size distribution of the aerosol. That is to say, smaller particles are more easily deposited in all regions of the human respiratory tract.

The total particle number deposition fraction in the human airways was estimated as 1.85×10^9 N cm^{-3}, 2.76×10^9 N cm^{-3} and 2.94×10^9 N cm^{-3} for the cigarette, e-cigarette and HnB product, respectively. Thus, the total number deposition fraction was comparable between the e-cigarette and HnB product, and slightly lower for the 3R4F cigarette. Studies have shown that the smaller the particles, the more toxic the effects (Delfino *et al.*, 2010; Meng *et al.*, 2013), and that the NC has a greater impact on health (Penttinen *et al.*, 2001). Notably, the NC of all three aerosols was much higher than that of air aerosol in the most heavily polluted day (Li *et al.*, 2016).

Fig. 5 shows the distribution of particle number deposition fraction in different regions of the human respiratory tract by particle size. For all three tobacco products, the size distributions of NC exhibited a unimodal distribution, peaking at around 200, 25 and 50 nm for the 3R4F cigarette, e-cigarette and HnB product, respectively. Among the respiratory regions, deposition in the pulmonary region was the highest, accounting for 60% of total inhaled particles, while that in the head airways was the lowest. Comparing the NC size distribution of the three tobacco products, the number deposition fraction in the pulmonary and tracheobronchial regions was larger for the HnB product than for both the 3R4F cigarette and e-cigarette, while the opposite trend was observed in the head airways. The number deposition fraction had a similar peak value in the pulmonary region for the 3R4F cigarette and e-cigarette, but was higher in the head for the 3R4F cigarette and higher in the tracheobronchial region for the e-cigarette. The observed differences among the three types of product might be due to the mechanisms underlying particle deposition. The particles in 3R4F cigarette smoke are larger and thus more likely to be deposited in the head airway by impaction, whereas smaller particles can easily permeate into and deposit in the alveolar and pulmonary regions (Geiser *et al.*, 2005).

3.4 Deposition of Aerosol in the Human Lungs

The MPPD model was used to predict the deposition of aerosol in different parts of the human lungs. The lungs comprise the left lung and the right lung; the left lung is split by the oblique fissure into the upper and lower lobes, while the right lung is divided into upper, middle and lower lobes. Overall, the patterns of deposition in the different lung lobes were relatively consistent for
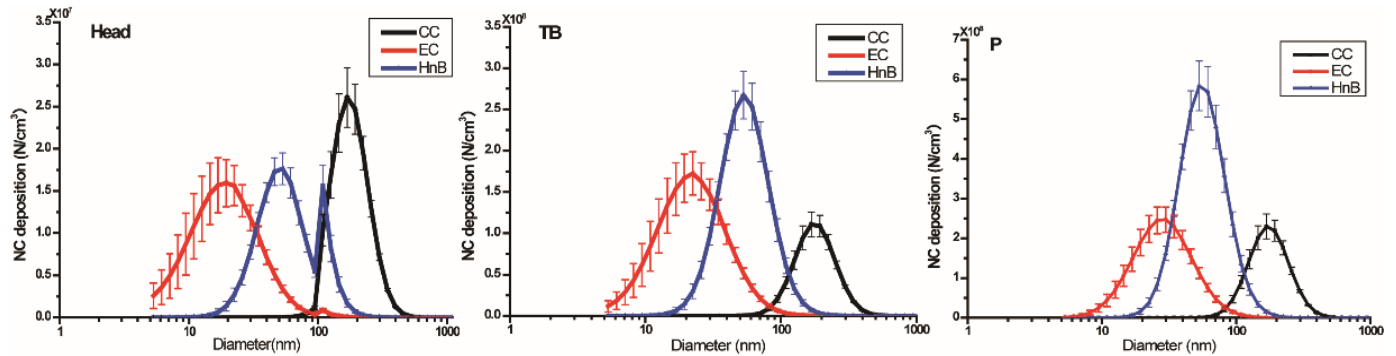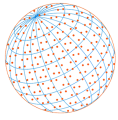
Fig. 5. Particle NC size deposition in the human airways for the CC, EC and HnB.
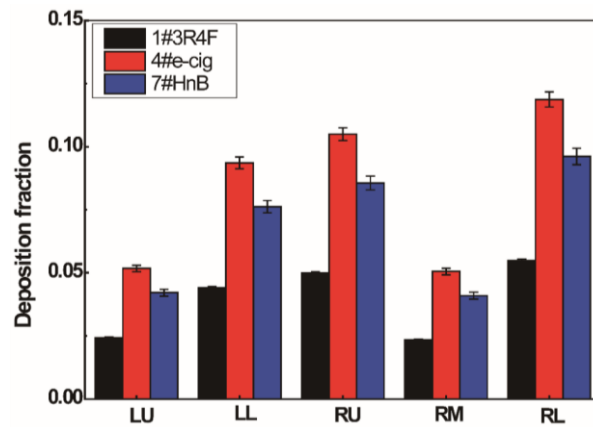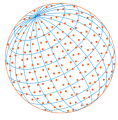

Fig. 6. Deposition fraction in different lobes of the lung for the three tobacco products. Abbreviations: LL, left lower lung lobe; LU, left upper lung lobe; RL, right lower lung lobe; RM, right middle lung lobe; RU, right upper lung lobe.

the 3R4F cigarette, e-cigarette and HnB cigarette, showing the following trend in deposition trend fraction: left upper lobe ≈ right middle lobe < left lower lobe < right upper lobe < right lower lobe. This trend is mainly related to the position of each lung lobe and the aerosol flow path. Among them, the left lower lobe has the longest flow path and a longer aerosol residence time, so it has a relatively higher deposition.

More specifically, as showed in Fig. 6, the deposition fraction was highest in the right lower lobe (0.055, 0.12, and 0.096 for the 3R4F cigarette, e-cigarette and HnB product, respectively), accounting for about 28% of the total lung lobe deposition fraction in each case. Furthermore, the deposition fraction in the left lower, right upper and right lower lobe generally accounted for 75% of the total lung lobe deposition fraction. For all three tobacco products, therefore, the aerosol was mainly deposited in the right lower lobe, the right upper lobe and the left lower lobe of the lung. We compared the deposition fraction of the aerosols in the different lobes of the lungs among the three products. Across all five lung lobes, the deposition fraction followed the order: e-cigarette > HnB cigarette > 3R4F cigarette; in particular, for the e-cigarette, the deposition fraction in the right lower lobe was 1.23 and 2.16 times higher than that of the HnB product and 3R4F cigarette, respectively. The difference in deposition fraction among the lung lobes mainly stems from variations in lobe structure. The right lower lung lobe, which has more and longer bronchial passages, tends to have a higher deposition fraction.

Because the deposition fraction was highest in the right lower lobe for all products, we used this lobe as an example to investigate the particle size distribution of NC among the three products. The 3R4F cigarette, e-cigarette and HnB product had different particle NC size deposition distributions, peaking at about 200 nm, 25 nm and 50 nm, respectively; and the peak value of the HnB product was higher than that of the 3R4F cigarette and e-cigarette, while the 3R4F cigarette had the smallest peak value (Fig. 7).

The airways of the lungs comprise bronchial trees formed by thousands of branches; each bronchus in the lungs is then repeatedly branched into numerous bronchioles, which are further expanded into capsules to form alveoli. The MPPD model was used to simulate the deposition of aerosols in different generations of the airways in human lungs.

On the whole, the deposition patterns of aerosol from the 3R4F cigarette, e-cigarette and HnB product in different generations of airway were consistent (Fig. 8). The deposition fraction showed the trend of a rise followed by a decline in deposition with the increase in airway generation. The peak deposition fraction varied among the different lung lobes, but peak deposition mainly occurred in the 20th to 24th generation airways (20th in the left upper; 23rd in the right middle,
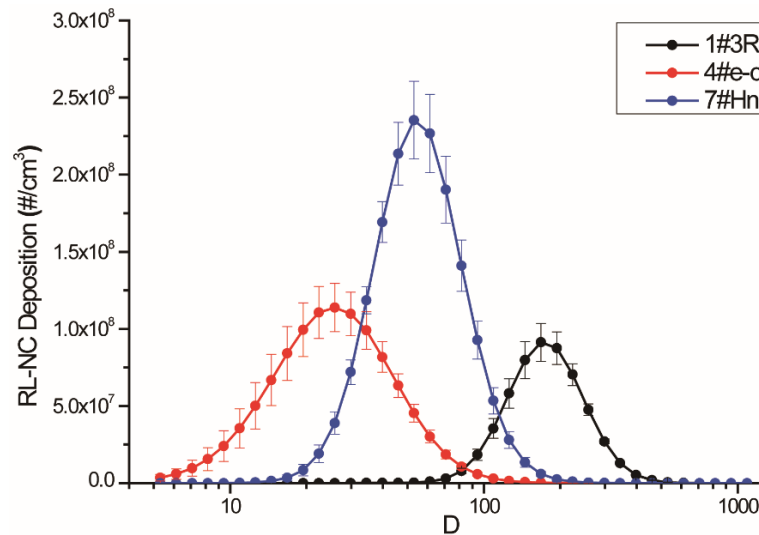

Fig. 7. Distribution of particle NC size deposition in the right lower (RL) lung lobe for the three tobacco products.
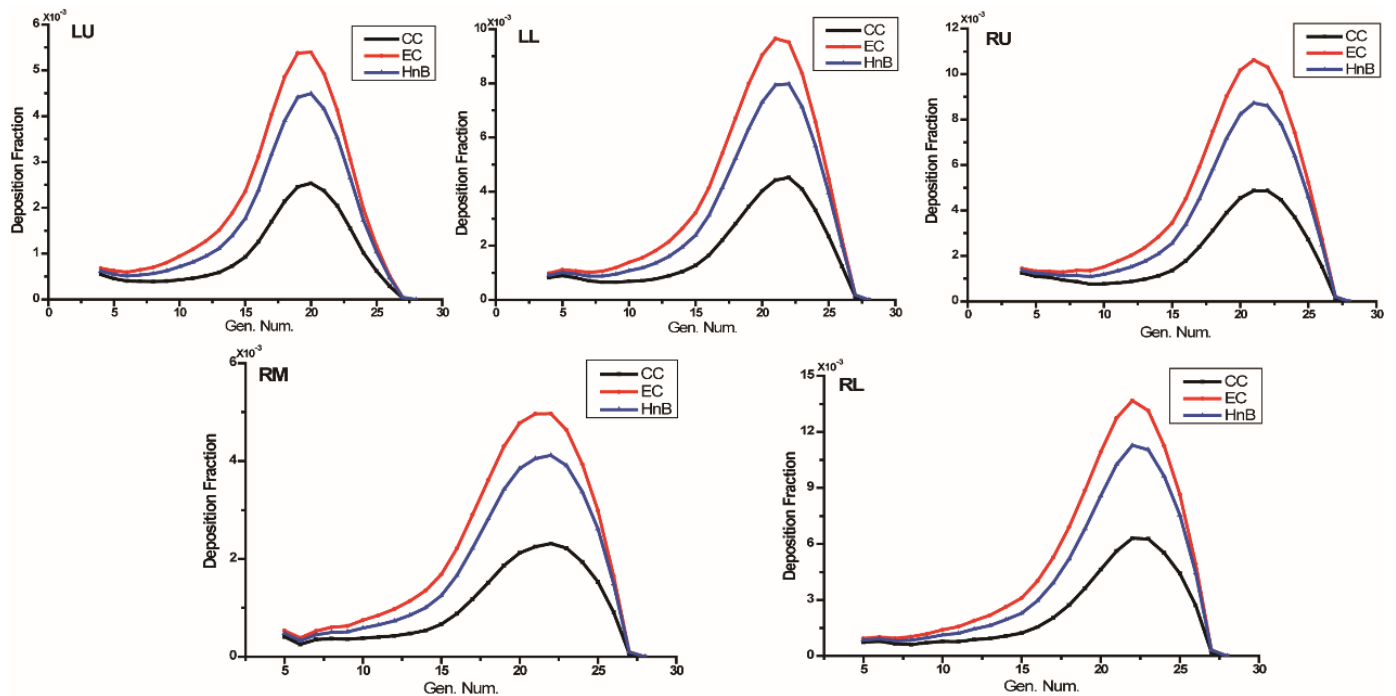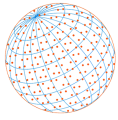

Fig. 8. Distribution of particle deposition fraction in increasing airway generations for the three tobacco products. (a) CC; (b) EC; (c) HnB. Abbreviations: LL, left lower lung lobe; LU, left upper lung lobe; RL, right lower lung lobe; RM, right middle lung lobe; RU, right upper lung lobe.

right upper and left lower; and 24th in right lower), which is consistent with a previous study (Manigrasso *et al.*, 2015). The peak value was highest in the right lower lobe, and decreased in the following order: right lower > right upper > left lower > left upper > right middle. The total deposition fraction for the three tobacco product aerosols in the different airway generations of the lungs showed the trend: e-cigarette > HnB product > 3R4F cigarette. Comparing the deposition fraction among the three products, the e-cigarette and HnB product had a much higher deposition fraction relative to the 3R4F cigarette, which is probably due to the smaller aerosol particles of the e-cigarette and HnB product.

4 CONCLUSION

In the present study, the physical properties of aerosols generated by conventional cigarettes, e-cigarettes and HnB products were compared by DMS-SCS. The measured data were then applied to the MPPD model to predict the distribution and deposition of the types of aerosol in different regions of the human respiratory tract (head airway, tracheobronchial, pulmonary) and different lobes of the human lungs. The model showed that the deposition fraction of the e-cigarette aerosol in the three regions of the human airway was higher than that of the HnB product and 3R4F cigarette. Among the three airway regions, the NC of deposited particles was highest in the pulmonary region; and the particle number deposition fraction of the e-cigarette and HnB product was higher than that of the 3R4F cigarette. The deposition fraction of smoke in different lung lobes also differed significantly: the deposition fraction was the highest in the right lower lobe for all three tobacco products. In terms of airway generation, the deposition fraction peaked in the 20th to 24th generation airways of the lobes. The particle NC size distributions in the lung lobes and airway generations were basically in line with the airway regions.

Regarding the three tobacco products, the aerosol from the e-cigarette and HnB product had a higher deposition fraction both in total and in each of the three respiratory regions. In other words, even though the aerosols from the e-cigarette and HnB product do not contain toxic components similar to those present in the aerosol from a conventional cigarette, there remains a risk of using e-cigarettes and HnB products due to the higher deposition fraction. It should be noted that the smoke aerosol used for deposition modeling was generated by SCS under the standard puffing regime, which is different from the real inhalation patterns of smokers. The real inhalation patterns with various puffing topographies may influence the size of particles and further influence the regional deposition in the respiratory system. Research into the deposition of tobacco product aerosol in the human respiratory tract, combined with knowledge of the harmful constituents of the aerosol, will provide important information for risk assessment of the inhalation toxicology for humans using cigarette and new tobacco products. In addition, based on the distribution of nicotine in the gas/particle phase, the aerosol deposition results can be used to evaluate nicotine transfer in individuals using tobacco products.
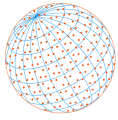
ACKNOWLEDGMENT

NOTES

The authors declare no competing financial interest.

SUPPLEMENTARY MATERIAL

Supplementary data associated with this article can be found in the online version at https://doi.org/10.4209/aaqr.200241
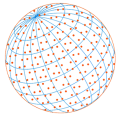
REFERENCES

Adam, T., McAughey, J., McGrath, C., Mocker, C., Zimmermann, R. (2009). Simultaneous on-line size and chemical analysis of gas phase and particulate phase of cigarette mainstream smoke. Anal. Bioanal. Chem. 394, 1193–1203. https://doi.org/10.1007/s00216-009-2784-y

Alderman, S.L., Ingebrethsen, B.J. (2011). Characterization of mainstream cigarette smoke particle size distributions from commercial cigarettes using a DMS500 fast particulate spectrometer and smoking cycle simulator. Aerosol Sci. Technol. 45, 1409–1421. https://doi.org/10.1080/02786826.2011.596862

Anjilvel, S., Asgharian, B. (1995). A multiple-path model of particle deposition in the rat lung. Fundam. Appl. Toxicol. 28, 41–50. https://doi.org/10.1006/faat.1995.1144

Asgharian, B., Price, O.T., Rostami, A.A., Pithawalla, Y.B. (2018). Deposition of inhaled electronic cigarette aerosol in the human oral cavity. J. Aerosol Sci. 116, 34–47. https://doi.org/10.1016/j.jaerosci.2017.11.014

Asgharian, B., Price, O.T., Yurteri, C. ., Dickens, C., Mcaughey, J. (2014). Component-specific, cigarette particle deposition modeling in the human respiratory tract. Inhalation Toxicol. 26, 36–47. https://doi.org/10.3109/08958378.2013.851305

Bair, W. (1995). The ICRP human respiratory tract model for radiological protection. Radiat. Prot. Dosim. 60, 307–310. https://doi.org/10.1093/oxfordjournals.rpd.a082732

Baker, R.R. (2006). Smoke generation inside a burning cigarette: Modifying combustion to develop cigarettes that may be less hazardous to health. Prog. Energy Combust. Sci. 32, 373–385. https://doi.org/10.1016/j.pecs.2006.01.001

Barua, R.S., Ambrose, J.A. (2013). Mechanisms of coronary thrombosis in cigarette smoke exposure. Arterioscler. Thromb. Vasc. Biol. 33, 1460–1467. https://doi.org/10.1161/ATVBAHA.112.300154

Boue, S., Goedertier, D., Hoeng, J., Kuczaj, A., Majeed, S., Mathis, C., May, A., Phillips, B., Peitsch, M. C., Radtke, F., Schlage, W.K., Tan, W.T., Vanscheeuwijck, P. (2020). State-of-the-art methods and devices for the generation, exposure, and collection of aerosols from heat-not-burn tobacco products. Toxicol. Res. Appl. 4, 1–40. https://doi.org/10.1177/2397847319897869

Broday, D.M., Robinson, R. (2003). Application of cloud dynamics to dosimetry of cigarette smoke particles in the lungs. Aerosol Sci. Technol. 37, 510–527. https://doi.org/10.1080/02786820300969

Carvalho, T.C., Peters, J.I., Williams III, R.O. (2011). Influence of particle size on regional lung deposition–What evidence is there? Int. J. Pharm. 406, 1–10. https://doi.org/10.1016/j.ijpharm.2010.12.040

Chen, C. (2017). Change and challenge: Outlook for development of new tobacco products. Acta Tabacaria Sin. 23, 14–18. https://doi.org/10.16472/j.chinatobacco.2017.082

Church, T.R., Anderson, K.E., Caporaso, N.E., Geisser, M.S., Le, C.T., Zhang, Y., Hecht, S.S. (2009). A prospectively measured serum biomarker for a tobacco-specific carcinogen and lung cancer in smokers. Cancer Epidemiol. Biomarkers. Prev. 18, 260–266. https://doi.org/10.1158/1055-9965

Cui, H., Yurteri, C.U., Cabot, R., Xie, F., Liu, H. (2020). Characterization of mainstream cigarette smoke aerosol by size-fractionated chemical analysis of nicotine, solanesol, and tobacco-specific nitrosamines. Part. Sci. Technol. 38, 587–595. https://doi.org/10.1080/02726351.2019.1567636

Delfino, R.J., Staimer, N., Tjoa, T., Arhami, M., Polidori, A., Gillen, D.L., Sioutas, C. (2010). Association of biomarkers of systemic inflammation with organic components and source tracers in quasi-ultrafine particles. Environ. Health Perspect. 118, 756–762. https://doi.org/10.1289/ehp.0901407

Duan, Y., Zhao, W., Yang, J., Han, J., Sun, Z., Yang, L., Chen, Y. (2015). Research on particle size distribution in traditional cigarette and electronic cigarette smoke aerosols. Acta Tabacaria Sin. https://doi.org/10.16472/j.chinatobacco.2014.298

Geiser, M., Rothen-Rutishauser, B., Kapp, N., Schürch, S., Kreyling, W., Schulz, H., Gehr, P. (2005). Ultrafine particles cross cellular membranes by nonphagocytic mechanisms in lungs and in cultured cells. Environ. Health Perspect. 113, 1555–1560. https://doi.org/10.1289/ehp.8006
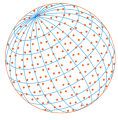
Geiss, O., Kotzias, D. (2007). Tobacco, cigarettes and cigarette smoke - An overview. EUR – Scientific and Technical Research Series. Office for Official Publications of the European Communities, Luxembourg. http://publications.jrc.ec.europa.eu/repository/bitstream/JRC37472/7472%20-%20EUR22783EN_Geiss_Kotzias.pdf

Hackshaw, A., Morris, J.K., Boniface, S., Tang, J.L., Milenković, D. (2018). Low cigarette consumption and risk of coronary heart disease and stroke: meta-analysis of 141 cohort studies in 55 study reports. BMJ 360, j5855. https://doi.org/10.1136/bmj.j5855

Hinds, W.C. (1978). Size characteristics of cigarette smoke. Am. Ind. Hyg. Assoc. J. 39, 48–54. https://doi.org/10.1080/0002889778507712

Hinds, W.C. (1999). Aerosol technology: Properties, behavior, and measurement of airborne particles. John Wiley and Sons.

Hofmann, W. (2011). Modelling inhaled particle deposition in the human lung—A review. J. Aerosol Sci. 42, 693–724. https://doi.org/10.1016/j.jaerosci.2011.05.007

Holmberg, R., Yeatts, L. (1976). Particle size distribution of mainstream tobacco and marijuana smoke. Analysis using the electrical aerosol analyzer. Am. Rev. Respir. Dis. 140, 202–205. https://doi.org/10.1164/ajrccm/140.1.202

International Organization for Standardization (ISO) (2000). ISO 3308: 2000-04-15: Routine Analytical Cigarette-smoking Machine--Definition and Standard Conditions. International Organization for Standardization. https://www.iso.org/standard/28325.html

International Organization for Standardization (ISO) (2018). ISO 20768:2018 I. Vapour products — Routine analytical vaping machine — Definitions and standard conditions. International Organization for Standardization. https://www.iso.org/standard/69019.html

Johnson, T.J., Olfert, J.S., Cabot, R., Treacy, C., Yurteri, C.U., Dickens, C., Symonds, J.P. (2015). Transient measurement of the effective particle density of cigarette smoke. J. Aerosol Sci. 87, 63–74. https://doi.org/10.1016/j.jaerosci.2015.05.006

Kane, D.B., Asgharian, B., Price, O.T., Rostami, A., Oldham, M.J. (2010). Effect of smoking parameters on the particle size distribution and predicted airway deposition of mainstream cigarette smoke. Inhalation Toxicol. 22, 199–209. https://doi.org/10.3109/08958370903161224

Kijowski, J. (1985). A review of particle size studies on cigarette smoke. Product Design MSA Collection. https://www.industrydocuments.ucsf.edu/docs/spbk0037

Kleinstreuer, C., Zhang, Z. (2010). Airflow and particle transport in the human respiratory system. Annu. Rev. Fluid Mech. 42, 301–334. https://doi.org/10.1146/annurev-fluid-121108-145453

Kleinstreuer, C., Feng, Y. (2013). Computational analysis of non-spherical particle transport and deposition in shear flow with application to lung aerosol dynamics--A review. J. Biomech. Eng. 135, 021008. https://doi.org/10.1115/1.4023236

Leaderer, B.P., Cain, W.S., Isseroff, R., Berglund, L.G. (1984). Ventilation requirements in buildings—II. Particulate matter and carbon monoxide from cigarette smoking. Atmos. Environ. 18, 99–106. https://doi.org/10.1016/0004-6981(84)90232-4

Li, X., Yan, C., Patterson, R.F., Zhu, Yujiao, Yao, X., Zhu, Yifang, Ma, S., Qiu, X., Zhu, T., Zheng, M. (2016). Modeled deposition of fine particles in human airway in Beijing, China. Atmos. Environ. 124, 387–395. https://doi.org/10.1016/j.atmosenv.2015.06.045

Liang, J.S., An, J.L., Wang, H.L., Zhang, Y.X., Wang, J.X., Shi, S.S., Wang, X. (2017). Modeled deposition of fine particles in human airway in northern suburb of Nanjing. Huan Jing Ke Xue 38, 1743–1752. https://doi.org/10.13227/j.hjkx.201610040

Manigrasso, M., Buonanno, G., Fuoco, F.C., Stabile, L., Avino, P. (2015). Aerosol deposition doses in the human respiratory tree of electronic cigarette smokers. Environ. Pollut. 196, 257–267. https://doi.org/10.1016/j.envpol.2014.10.013

Martins, L.D., Martins, J.A., Freitas, E.D., Mazzoli, C.R., Goncalves, F.L., Ynoue, R.Y., Andrade, M.D. (2010). Potential health impact of ultrafine particles under clean and polluted urban atmospheric conditions: A model-based study. Air Qual. Atmos Health 3, 29–39. https://doi.org/10.1007/s11869-009-0048-9

McCusker, K., Hiller, F., Wilson, J., McLeod, P., Sims, R., Bone, R. (1982). Dilution of cigarette smoke for real time aerodynamic sizing with a SPART analyzer. J. Aerosol Sci. 13, 103–110. https://doi.org/10.1016/0021-8502(82)90055-6

Mellat, M., Momtazi Borojeni, A. A., Sahebkar, A., Ghanei, M. (2017). Adapting the ICRP model to predict regional deposition of the pharmaceutical aerosols inhaled through DPIs and nebulizers.
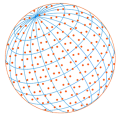
J. Drug Delivery Sci. Technol. 37, 81–87. https://doi.org/10.1016/j.jddst.2016.12.002

Meng, X., Ma, Y., Chen, R., Zhou, Z., Chen, B., Kan, H. (2013). Size-fractionated particle number concentrations and daily mortality in a Chinese city. Environ. Health Perspect. 121, 1174–1178. https://doi.org/10.1289/ehp.1206398

Miller, F.J., Asgharian, B., Schroeter, J.D., Price, O. (2016). Improvements and additions to the Multiple Path Particle Dosimetry model. J. Aerosol Sci. 99, 14–26. https://doi.org/10.1016/j.jaerosci.2016.01.018

Patterson, R.F., Zhang, Q., Zheng, M., Zhu, Y. (2014). Particle deposition in respiratory tracts of school-aged children. Aerosol Air Qual. Res, 14, 64–73. https://doi.org/10.4209/aaqr.2013.04.0113

Penttinen, P., Timonen, K., Tiittanen, P., Mirme, A., Ruuskanen, J., Pekkanen, J. (2001). Ultrafine particles in urban air and respiratory health among adult asthmatics. Eur. Respir. J. 17, 428–435. https://doi.org/10.1183/09031936.01.17304280

Pichelstorfer, L., Hofmann, W., Winkler-Heil, R., Yurteri, C.U., McAughey, J. (2016). Simulation of aerosol dynamics and deposition of combustible and electronic cigarette aerosols in the human respiratory tract. J. Aerosol Sci. 99, 125–132. https://doi.org/10.1016/j.jaerosci.2016.01.017

Protano, C., Manigrasso, M., Avino, P., Vitali, M. (2017). Second-hand smoke generated by combustion and electronic smoking devices used in real scenarios: Ultrafine particle pollution and age-related dose assessment. Environ. Int. 107, 190–195. https://doi.org/10.1016/j.envint.2017.07.014

Rodgman, A., Perfetti, T.A. (2008). The Chemical Components of Tobacco and Tobacco Smoke. CRC Press. https://doi.org/10.1201/9781420078848.

Rostami, A.A. (2009). Computational modeling of aerosol deposition in respiratory tract: A review. Inhalation Toxicol. 21, 262–290. https://doi.org/10.1080/08958370802448987

Roy, M., Becquemin, M., Bouchikhi, A. (1991). Ventilation rates and lung volumes for lung modelling purposes in ethnic groups. Radiat. Prot. Dosim. 38, 49–55. https://doi.org/10.1093/rpd/38.1-3.49

Sahu, S.K., Tiwari, M., Bhangare, R.C., Pandit, G.G. (2013). Particle size distribution of mainstream and exhaled cigarette smoke and predictive deposition in human respiratory Tract. Aerosol Air Qual. Res. 13, 324–332. https://doi.org/10.4209/aaqr.2012.02.0041

Si, X., Tang, J., Zhu, R., Han, J., You, J., Li, Z., Jiang, W., Su, Z., Miao, M., Liu, Z. (2018). Aerosol particle size distribution from an electrical heat-not-burn product under ISO and HCI smoking regimes. Tobacco Sci. Technol. 21, 47–52. https://doi.org/10.16135/j.issn1002-0861.2017.0501

Simonavicius, E., McNeill, A., Shahab, L., Brose, L.S. (2019). Heat-not-burn tobacco products: A systematic literature review. Tobacco Control 28, 582–594. https://doi.org/10.1136/tobaccocontrol-2018-054419

Sosnowski, T.R. (2011). Importance of airway geometry and respiratory parameters variability for particle deposition in the human respiratory tract. J. Thorac. Dis, 3, 153–155. https://doi.org/10.3978/j.issn.2072-1439.2011.06.01

Sosnowski, T.R., Kramek-Romanowska, K. (2016). Predicted Deposition of e-cigarette aerosol in the human lungs. J. Aerosol Med. Pulm. Drug Delivery 29, 299–309. https://doi.org/10.1089/jamp.2015.1268

Sosnowski, T.R., Odziomek, M. (2018). Particle size dynamics: toward a better understanding of electronic cigarette aerosol interactions with the respiratory system. Front. Physiol. 9, 853. https://doi.org/10.3389/fphys.2018.00853

Symonds, J.P., Reavell, K.S.J., Olfert, J.S., Campbell, B.W., Swift, S.J. (2007). Diesel soot mass calculation in real-time with a differential mobility spectrometer. J. Aerosol Sci. 38, 52–68. https://doi.org/10.1016/j.jaerosci.2006.10.001

U.S. Department of Health and Human Services (2014). The Health Consequences of Smoking— 50 Years of Progress: A Report of the Surgeon General. U.S. Department of Health and Human Services, Centers for Disease Control and Prevention, National Center for Chronic Disease Prevention and Health Promotion, Office on Smoking and Health. https://www.ncbi.nlm.nih.gov/books/NBK294315/

World Health Organization (WHO) (2008). WHO report on the global tobacco epidemic, 2008: The MPOWER package. World Health Organization. https://www.who.int/tobacco/mpower/2008/en

Zhang, Y., Sumner, W., Chen, D.R. (2012). In vitro particle size distributions in electronic and

conventional cigarette aerosols suggest comparable deposition patterns. Nicotine Tob. Res. 15, 501–508. https://doi.org/10.1093/ntr/nts165

Zhe, Z., Kleinstreuer, C., Hyun, S. (2012). Size-change and deposition of conventional and composite cigarette smoke particles during inhalation in a subject-specific airway model. J. Aerosol Sci. 46, 34–52. https://doi.org/10.1016/j.jaerosci.2011.12.002